Abstract

Metabolic effects of *skn-1* down-regulation in *C.elegans*

Phan Chau Hong Duc
Natural Products Science Major
College of Pharmacy
The Graduate School
Seoul National University

SKN-1/Nrf2, a transcription factor with a well-established role in regulating oxidative stress resistance and detoxification pathway, has also been proved to affect the lifespan of *C.elegans*. While many studies have characterized the SKN-1 function at genomic level, there has been lack of a systematic investigation at individual metabolites. As SKN-1 function relates to metabolism, we studied metabolite profiles of *skn-1* knockdown *C.elegans* strain by NMR and LC-MS/MS metabolomics approach. First, we fed *C.elegans* with *E.coli* HT115 containing the double-strand RNA of *skn-1* to knock down *skn-1* gene in the worms. The effects

of *skn-1* knockdown were confirmed by the shorter lifespan and the lower level of *skn-1* expression measured by qPCR in knockdown worms. We then extracted metabolites from the worms and obtained metabolite profiles through NMR and LC-MS/MS. Multivariate analysis showed a distinctive metabolic profile with the significant decrease in the oxidative stress defense system represented by the reduction in NADPH/$NADP^+$ ratio, the decline in the transsulfuration pathway-main source of GSH synthesis, and the lower level of total GSH (GSHt) in *skn-1* RNAi worms. We also tested the performance of phase II detoxification system since we previously observed the involvement of the *skn-1* dependent phase II detoxification in the dietary restriction′s beneficial effects. It is showed that there is an impairment of this system in the knockdown worms as exemplified by the lower level of glutathione conjugate of paracetamol, a compound detoxified through this pathway. By interrogating existing microarray data, we also observed the consistency in the changes of metabolite data with the gene expression levels, including the decline of *cbl-1* and *gpx* encoding gamma-cystathionase and glutathione peroxidase which are necessary for the synthesis and function of GSH respectively, the reduction in the T25B9.9 encoding 6-gluconate phosphate dehydrogenase, which is the main enzyme of NADPH production, and the decrease of *ugt* and *gst* encoding UDP-glucuronosyl transferase and Glutathione-S-transferase in the Phase II detoxification pathway. As the correlation between aging and oxidative damage has been hypothesized previously, our results demonstrate the debilitation of the cytoprotective pathway including oxidative stress defense

system and xenobiotic detoxification system, underlies the lifespan reduction of *skn-1* knockdown worms.

Keywords: *skn-1*, phase II detoxification, *C.elegans*, metabolomics

Student number: 2013-22584

Table of Contents

List of Figures

List of Tables

I. Introduction

SKN-1/Nrf2 transcription factor belongs to the cap'n'collar family that mediates an evolutionarily conserved oxidative stress resistance in mice (1), zebra fish (2), nematode (3), (4), and flies (5). In addition, Nrf2 has been proposed to be a potential target for cancer chemoprevention (6) (7). In aging research, while the relationship between Nrf2 and lifespan in vertebrate organisms such as mice, zebra fish remains controversial (8) (2), the implementation of Nrf2 ortholog SKN-1 in lifespan of *C.elegans* is well documented (3). The expression of *skn-1* in ASI neurons necessitated lifespan extension in worms under caloric restriction (9) and knockdown of *skn-1* gene by RNA interference (*RNAi*) was shown to reduce the worm's lifespan by 20 % (10). Recently, SKN-1 was reported to interact with Insulin/IGF-1-signaling pathway in stress tolerance and longevity promotion (11), suggesting the important role of SKN-1 in cellular metabolism.

One of the most critical functions of SKN-1/Nrf2 is to regulate the expression of phase II detoxification enzyme (12) (13). This detoxification system is necessary for the survival of *C.elegans* in the natural environment. There is a large number of genes encoding major enzymatic tools of phase II detoxification in worms, including Glutathione-S-transferase (GSTs) and UDP-glucuronosyl transferase (UGTs) (14). These enzymes catalyze conjugation reactions between phase II metabolites and charge species such as glutathione or glucuronic acid to enhance the elimination of toxic insults such as reactive oxygen species and electrophiles

(15) (16). In response to oxidative stressors, adult worms up-regulate the expression of various antioxidant genes such as GSTs, catalase, superoxide dismutase in a SKN-1-dependent manner (17). Thus, the dual function of SKN-1 in both longevity and cytoprotection has raised possibility of the correlation of two pathways, which has not been fully understood (18) (19).

Most studies of SKN-1 hitherto have focused mainly on its function at genomic level. The understanding of SKN-1 role in cellular metabolism, indeed, remains incomplete. As metabolite profiling directly reflects the activity of metabolic network, metabolomics approach has increasingly been applied to investigate the metabolic alterations under experimental perturbations (20). In *C.elegans* model, ^{1}H nuclear magnetic spectroscopy has been employed so far to characterize the metabolites of many long-lived *C.elegans* (21) (22) (23). However, the overlapping of the signals makes it difficult to identify and quantify metabolites (24). This limitation can be overcome by using heteronuclear multidimensional NMR with stable isotope labeling (25). This method has been applied for many organism models such as bacteria, silkworm, and mice (26).

Our previous study the first time reported an *in vivo* ^{13}C-labeling strategy of all metabolites in *C.elegans* with improving the sensitivity of 2 order magnitudes and increasing the number of detectable peaks (27). Herein, we apply the ^{13}C-labeling method to examine the metabolic alterations in *skn-1* knockdown *C.elegans* by two-dimensional NMR combining with LC/MS. To characterize the changes of phase II detoxification metabolites in these worms, we treated *C.elegans* to

paracetamol, a compound detoxified through phase II enzymes and monitored its metabolites by HPLC-Mass spectroscopy. Our results show the distinctive metabolic profile with the significant increase in the phosphocholine and AMP/ATP ratio, potential biomarkers of aging, together with the decrease in GSHt and NADPH/NADP ratio, indicating the deterioration in oxidative stress defense system in *skn-1* knockdown worms. The paracetamol metabolites through the Phase II detoxification are diminished, suggesting a decline in the performance of this system. By interrogating the existing gene expression data, we find high concordance between transcriptional and metabolite changes. These alterations reflect the defective in the cytoprotective pathway, explaining for the lifespan reduction in the *skn-1* knockdown *C.elegans*.

II. Materials and Methods

1. ^{13}C-labeling metabolites and RNAi

NGM plates were prepared as previous study (27). An autoclaved mixture containing of NaCl (1.5 g), agar (10 g) dissolved in 484 mL of distilled water was additionally added ^{13}C6-glucose (1 g), NH_4Cl (1 g), 1 M CaCl2 (0.5 mL), 1 M $MgSO_4$ (0.5 mL), 1% (v/v) thiamine (0.5 mL), cholesterol 5 mg mL^{-1} (2 mL), 1 M KH_2PO_4 pH 6.0 buffer (12.5 mL), and ampicillin (X1000, 500 μL). This agar solution was used to make 100 mm plastic Petri dish plates. The RNAi was performed as describing previously (28). *E.coli* HT115 carrying L4440 vector that expressed either *skn-1* dsRNA or nothing as control was initially grown at 37 ^{0}C in LB media overnight. 10 ml LB media was subsequently added to 1 L M9 buffer composed of NaH_2PO_4 (6.8 g), K_2HPO_4 (3 g), NaCl (0.25 g), a filtered mixture containing ^{13}C6-glucose (2 g), NH_4Cl (2 g), 1 M $CaCl_2$(100 μL), 1 M $MgSO_4$ (1 mL), 1% (v/v) thiamine (1 mL), and ampicillin (X1000, 1 mL) and continued culturing to OD_{600} = 0.4. 1M IPTG (800 μL) was added to cultured media for 1 hour to induce the expression of dsRNA. The cultured E.coli was harvested by centrifugation at 60000 rpm in 20 min at RT, and the pellet was resuspended in 50 mL culture media. 1ml of *E.coli* suspension was spread on to one agar plate and incubated at 37 ^{0}C overnight. Wild type *C.elegans* Bristol strain (N2) was used. A synchronous population of L1 larvae of wild type *C.elegans* Bristol strain (N2)

was placed on NGM plates at 20 ^{o}C until they reach adult. Adult *C.elegans* were then harvested for metabolite extraction.

2. Metabolite extraction

Adult *C.elegans* were harvested and lyzed with a tissue lyser bead mill (Biospec) in 600 μL methanol/chloroform mixture (2:1). Samples were vortexed for 50 s and incubated on ice for 10 s. This step repeated 5 times. Samples were subsequently sonicated for 10 min in cold water and additionally added 400 μL cholorform/water mixtures (1:1). After samples were centrifuged at 15000 g for 20 min at 4 ^{0}C, the upper water phase was separated and dried with a centrifugal evaporator (Vision). The protein precipitation was collected for BCA assay.

3. NMR acquisition and Data analysis

The dried water phase was rehydrated in 450 μL of NMR buffer (100% D_2O, 100 mM Potassium phosphate pH 7.0, 1 mM 4,4-dimethyl-4-silapentane-1-sulfonic), and transferred into a 5 mm NMR tube. The 2D – heteronuclear single quantum coherence (HSQC) experiment was carried out by a 600 MHz Bruker Advance spectrometer equipped with a cryogenic triple resonance probe at the Inter-university facility Department, Seoul National University (Seoul, Korea). The processing and analysis of HSQC data followed our previous paper (27). NMRViewJ software was used to process the NMR spectra, and the total peak volumes were used to normalize the integrated peak volumes. Orthogonal

projections to latent structures-discrimination analysis (OPLS-DA), class discrimination models and S-plot were performed by SIMCA-P 11.0 (Umetrics). Other statistical analysis was done on Origin software (Originlab).

4. LC-MS/MS – based targeted metabolomics

ATP, ADP, Glucose, Trehalose, NADPH, Citrate, Malate, GDP, GSH and GSSG concentrations in WT and *skn-1* RNAi *C.elegans* were measured on API2000 Mass spectrometer (AB/SCIEX) equipped with an electrospray ionization (ESI) source, and used in negative mode with −4.5 kV ion spray voltage and 300 °C heater (turbo) gas temperature. The dried water phase was dissolved in the mixture of Water: Methanol (20 μL, 1:1 v/v). 2 μL of the sample was injected into an HPLC (Agilent 1100 Series, Agilent, CO). Mobile phase, flow rate, and column were used as previous study (27). For each compound quantification, multiple reaction monitoring (MRM) was employed. The following transitions were monitored m/z = 506 → 159 for ATP, m/z = 426 → 159 for ADP, m/z = 178.8 → 88.9 for Glucose, m/z = 340.9 → 59 for Trehalose, m/z = 744.1 → 79 for NADPH, m/z = 190.8 → 11.1 for Citrate, m/z = 132.8 → 71 for Malate, m/z = 442 → 150 for GDP, m/z = 306 → 128 for GSH, and m/z = 611 → 306 for GSSG. The LC-MS/MS data were normalized by protein concentration measured by BCA method.

5. Normalization of LC/MS-MS data by protein concentration

The protein concentration is determined by bicinchoninic acid method (29) (BCA Protein Assay Kit, Pierce, USA, Prod#23227). The protein precipitation was dissolved in 1 M NAOH (180 µL) and heated at 70 ^{0}C for 25 min. Distilled water (1620 µL) was then added to dilute the base by ten times. The sample was mixed well by vortexing and was centrifuged at 15000 g for 5 min. The supernatant (10 µL) was used for BCA assay according to manufacturer's instruction.

6. Lifespan analysis

The first day of adulthood was set as t=0. Worms were cultured on *E.coli* HT115 carrying empty L4440 vector as control and L4440-*skn-1* vector as knockdown worms. Worms were transferred to new plates every day to prevent mixing with the progeny. The log-rank test employed to analyze the difference in the lifespan was performed on R software.

7. Real time Polymerase chain reaction (qPCR)

200 adult worms from each 3 biological independent replicate were collected and snap freezing in liquid nitrogen to extract RNA using Trizol method (MG^{TM} RNAzol, Macrogen, Cat. No. MR001S MR001L), followed by Phenol-Chloroform purification. RNA purity and concentration were assessed using the ratio of absorbance at 260 nm and 280 nm on NanoDrop 1000 spectrophotometer (ThermoScientific, Baltimore, MA, USA). cDNA was synthesized from 2 µg

RNA using High Capacity cDNA Reverse Transcription Kit (Lot No. 1304185, Applied Biosystems, Inc., USA). Real-time PCR reaction was performed in triplicate in an Applied Biosystems 7300 PCR machine with SYBR green –based detection (iTaq ^{TM} Universal SYBRR Green Supermix, Cat. No. 172-5120, Bio-Rad, USA). The gene expression ΔCt value of *skn-1* was calculated by normalization with *actin-1*. Statistical test was performed by Origin software (version 8, Microcal Software Inc., Northampton, MA). Primers were designed as follows:

skn-1 right GGCGCTACTGTCGATTTCTC;

skn-1 left CTCCATTCGGTAGAGGACCA;

act-1 right GCTTCAGTGAGGAGGACTGG;

act-1 left GTCGGTATGGGACAGAAGGA.

8. Gene expression analysis

Microarray data of the Oliveira et al.'s paper (12) were downloaded from the database PUMAdb (http://puma.princeton.edu). The data from experiment comparing gene expression in WT and *skn-1* RNAi on NGM plates were used to interrogate the expression level of genes encoding all metabolic enzymes in our study. KEGG database (http://www.kegg.jp/kegg/pathway.html) was used to identify genes and metabolic pathways in *C.elegans*. *p*-value was derived from Student *t*-test in Original software.

9. Targeting phase II detoxification metabolites

3500 adult worms were treated with Paracetamol (Sigma, Lot#SLBH0185V) for different time-points: 2, 6, and 10 hours. The phase II conjugates of paracetamol were extracted from *C.elegans* using the same protocol as metabolite extraction. Glutathione conjugate of paracetamol was quantified by AB Sciex API2000/Agilent 1100 series LC–MS/MS system with the same condition as previous study (27). The following transitions were monitored m/z = 457 → 140.1 for paracetamol - glutathione conjugate. Experiment was replicated three times.

III. Results

1. Effects of the *skn-1* knockdown on the *C.elegans*

RNA interference (RNAi) was used to knock down *skn-1* gene in *C.elegans*. Real-time Polymerase Chain Reaction (qPCR) was employed to compare the expression level of *skn-1* gene in knockdown strain and wild-type (WT). In *skn-1* RNAi strain, the expression level of *skn-1* reduced significantly by 70 % compared to WT (p-value $< 4.66 \times 10^{-4}$) (Figure 1.A). Knockdown of *skn-1* resulted in a significant lifespan decrease of *C.elegans* (p-value $< 3 \times 10^{-6}$) (Figure 1.B).

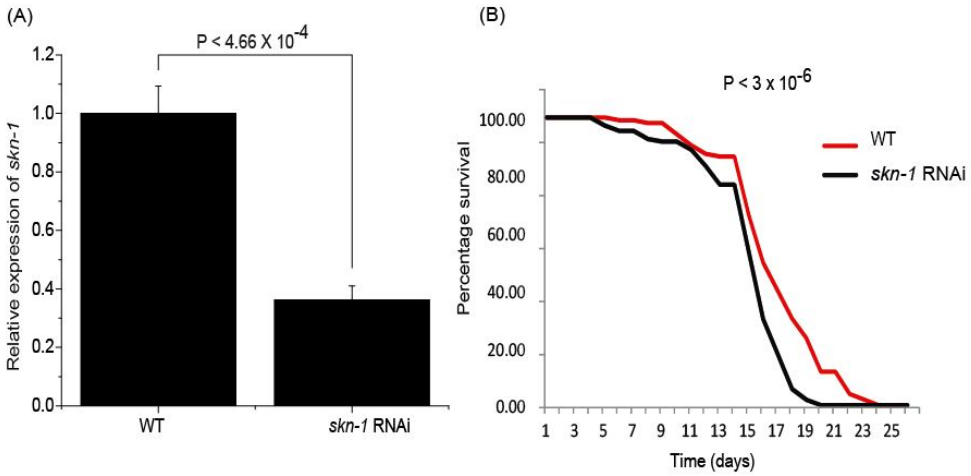

Figure 1. Real time PCR validation and lifespan confirmation

(A) Real time PCR validation. Gene expression level of *skn-1* in knockdown strain and WT. Error bars are standard deviation, *p-value* is derived from *Student-t* test, n = 3 trials. (B) Lifespan of *skn-1* RNAi *C.elegans* compared to WT (*p*-value is derived from log- rank test).

2. NMR-based metabolomic profiling of *skn-1* RNAi *C.elegans*

We performed a workflow of ^{13}C -labeling metabolites in *C.elegans* with ^{13}C-glucose. We then acquired the 2D-HSQC NMR spectra for the *skn-1* RNAi strain and WT. The spectra were quite similar and featured more than 250 resolved peaks (Figure 2A). The extracted one-dimensional spectra from the dotted lines showed the clear differences in peak intensities between two groups (Figure 2B).

Multivariate analysis was employed to study the differences between two groups. Orthogonal projections to latent structures-discriminant analysis (OPLS-DA) showed a clear separation between *skn-1* RNAi and WT. The model had one predictive and three orthogonal components with $Q^2(Y)=0.771$, $R^2(Y)=0.926$, and total $R^2(X)=0.712$ (Figure 3.A), suggesting that these two groups have distinct metabolite profiles. To identify peaks contributing to the difference, we constructed the S-plot based on the OPLS-DA model (Figure 3.B).

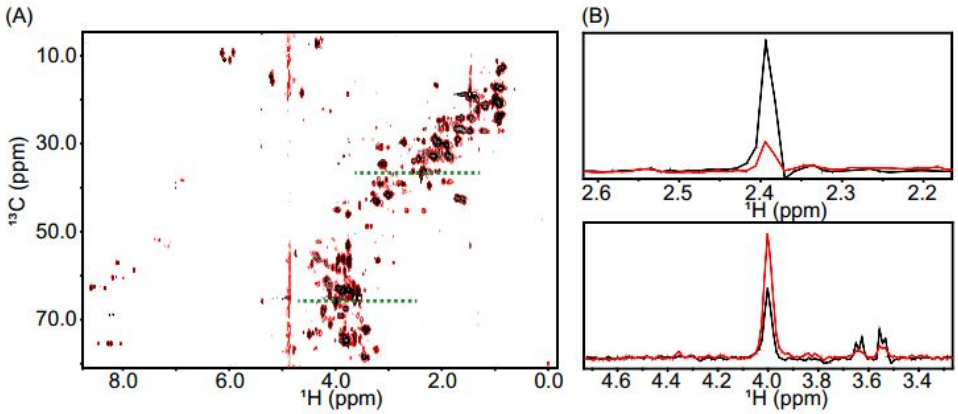

Figure 2. NMR spectra of WT and *skn-1* knockdown worms

(A) HSQC spectra for WT (black) and *skn-1* RNAi (red) are overlaid. (B) The extracted one-dimension spectra from the dotted lines indicated the differences in peak intensities

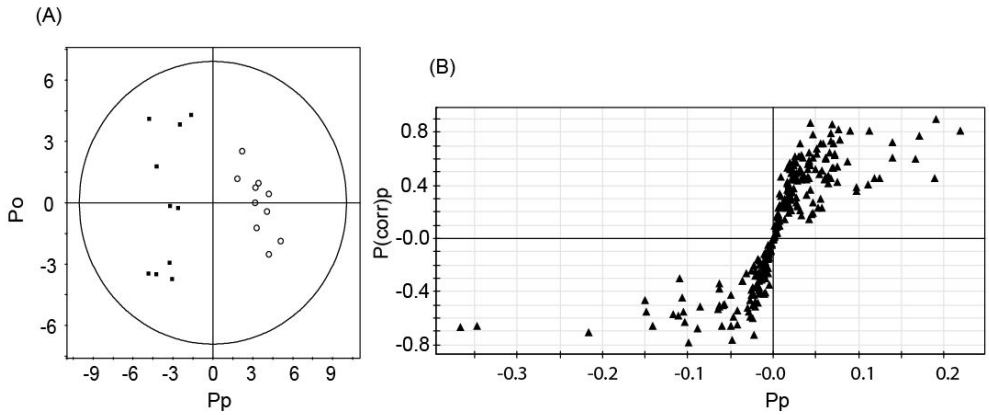

Figure 3. Multivariate analysis between WT and *skn-1* RNAi data.

(A) OPLS-DA score plot showing the different metabolite profiles between WT (filled box) and *skn-1* RNAi (open circle). (B) S-plot showing the peaks responsible for the discrimination.

3. Metabolite level changes combined with micro array data in *skn-1* RNAi *C.elegans*

We assigned the chemical shift values of significant peaks contributing to the difference using the SpinAssign (30) and calculated the fold change of the metabolite levels in *skn-1* RNAi compared to WT (Table 1). As there are some metabolites whose peaks were not clearly resolved in the NMR spectrum, these metabolite levels were confirmed by LC-MS/MS. In general, knockdown of *skn-1* resulted in the alterations of metabolites belonging to multiple pathways in *C.elegans* such as amino acid regulation (i.e., methionine, isoleucine, arginine, glutamine, glutamate ...), phospholipid regulation (i.e., ethanolamine, choline…), redox state regulation (i.e., ATP, AMP, NADPH, GSH, GSSG…). To cross-confirm our metabolite data with other approaches, we interrogated expression levels of genes encoding metabolic enzymes from the existing microarray data. Consistent with the metabolite data, the gene expression levels in comparable pathways were also changed. The reduction in expression level of T25B9.9 gene encoding enzyme 6-phosphogluconate dehydrogenase, an enzyme in the pentose phosphate pathway generating NADPH, explained for the low level of NADPH in knockdown worms. The decrease of GSH is commensurate with the reduction in the expression level of *cbl-1* gene, which encodes gamma-cystathionase in the GSH synthesis route (Figure 4). The expression levels of other genes are presented in Table 2.

Table 1. Changes of metabolites contributing to the difference between WT and *skn-1* RNAi

Metabolite	Fold Change (%)	*p*-value less than	Metabolite	Fold Change (%)	*p*-value less than
Ethanolamine phosphate	9.11	9.2×10^{-5}	L-glutamine	-12.00	0.0129
Ethanolamine	94.71	1.5×10^{-5}	L-glutamate	-10.60	0.0181
L-serine	54.18	1.88×10^{-6}	L-Lysine	-15.78	4.09×10^{-4}
sn-Glycerol 3-phosphate	55.28	4.3×10^{-4}	L-Cystathionine	-12.70	0.0206
Choline	43.53	7.22×10^{-7}	Pyruvate	-24.30	0.0117
Choline phosphate	33.62	0.0114	L-2-Aminoadipate	-22.10	0.0145
L-Methionine	51.87	9.15×10^{-5}	L-histidine	-13.45	0.0106
L-Isoleucine	19.02	4.13×10^{-4}	ADP*	-28.73	1.27×10^{-4}
Glycerone phosphate	115.70	0.0275	GDP*	-42.31	0.00234
L-Arginine	22.44	3.6×10^{-4}	NADPH*	-51.53	2.66×10^{-5}
Glucose *	40.09	1.66×10^{-4}	Citrate*	-39.49	6.42×10^{-5}
Trehalose*	61.92	4.62×10^{-4}	ATP*	-34.67	5.98×10^{-4}
AMP/ATP*	37.95	0.0183	GSHt*	-29.58	3.08×10^{-5}
			GSSG*	-24.44	2.11×10^{-3}
			Malate*	-26.33	0.0114
			NADPH/NADP	-44.83	6.73×10^{-3}

The change values are from the normalized peak volumes of the HSQC spectra and represent percent changes of *skn-1* RNAi compared to the WT with negative values for decrease and positive value for increase. The level of metabolites with * were confirmed by LC-MS/MS. GSHt = GSH + GSSG

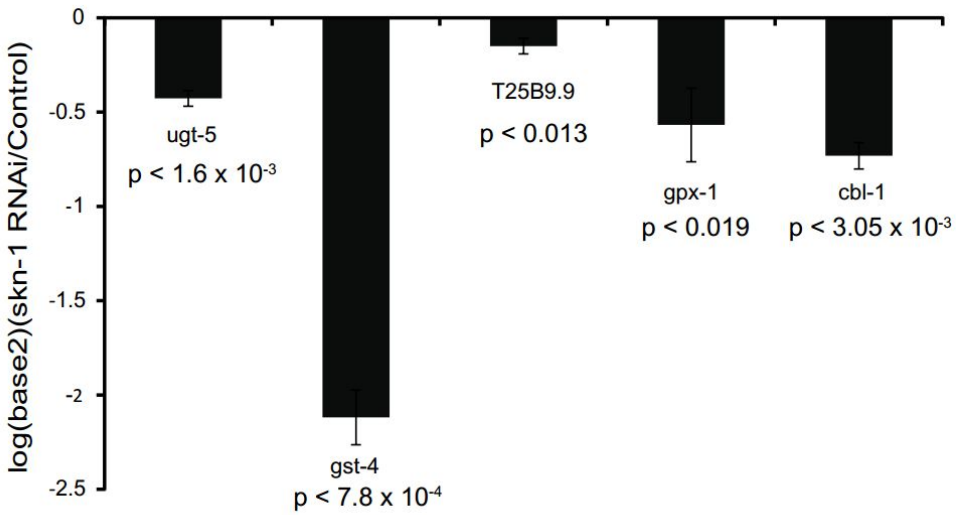

Figure 4. Gene expression level extracted from microarray data comparing *skn-1* RNAi and Control.

Representation of changed genes in *skn-1* knockdown worms. *ugt-5* : UDP-glucunosyltransferase; *gst-4* : Glutathione S- transferase; *gpx-1* : Glutathione peroxidase; T25B9.9: 6-phosphogluconate dehydrogenase; *cbl-1* : gamma-cystathionase. Error bars are Standard deviation, *p-value* is derived from *Student-t* test, n = 3 trials.

4. LC-MS/MS – based metabolomic targeting phase II detoxification metabolites

To assess the effect of *skn-1* on the phase II detoxification pathway in *C.elegans*, we treated *C.elegans* with paracetamol, a compound detoxified through this pathway, for different time-points: 2, 6, 10 hours, and quantified its phase II conjugates by LC-MS/MS. It clearly showed that at 2, and 6 hours, the paracetamol-glutathione conjugate level was reduced significantly in the *skn-1* RNAi worms comparing to WT (p-value < 0.03). At 10 hours, this level was not significant different between two groups. The decrease in the level of paracetamol-glutathione conjugate reflected the impairment in the phase II detoxification pathway, which is commensurate with the reduction of genes encode glutathione S-transferase such as *gst-4, gst-10*... (Figure 4, Table 2).

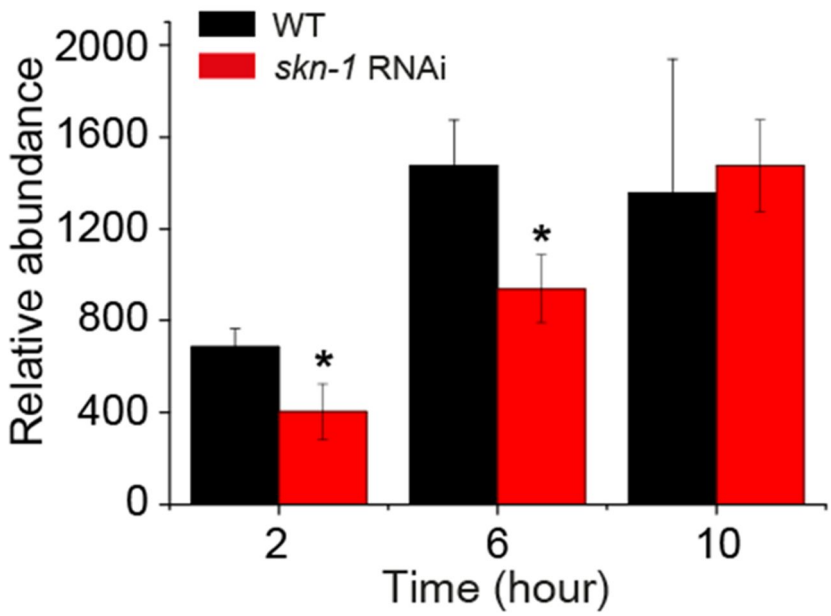

Figure 5. Paracetamol-glutathione conjugate level in *skn-1* knockdown worms comparing to WT

Level of Paracetamol-glutathione conjugate in WT and *skn-1* RNAi *C.elegans*. Statistical analysis was performed using Student's *t-test*; ***:** *p-value* < 0.03. Error bars are standard deviation.

IV. Discussion

Transcription factor SKN-1 with dual function in aging and oxidative stress resistance has attracted much attention. However, most of the studies have taken a genetic approach to define the role of *skn-1* gene. In order to have the more complete picture of *skn-1* function, we applied metabolomics approach to characterize the change in the metabolome of *skn-1* RNAi worms comparing to WT. We employed an *in vivo* ^{13}C-labeling metabolite workflow for *C.elegans* to increase the resolution and sensitivity of 2D HSQC NMR spectra. HPLC-MS/MS analysis was used to confirm the levels of metabolites which have many overlapping peaks in NMR spectra and to quantify the phase II detoxification conjugates of paracetamol.

The metabolomic profiling showed a significant decrease in the ratio of $NADPH/NADP^+$ in *skn-1* knockdown worms. As NADPH formation is involved in different processes, we retrieved gene expression level information from microarray data to have a thorough view of NADPH biosynthesis. One of the well-known enzyme groups generating NADPH belongs to pentose phosphate pathway with 2 enzymes Glucose-6-phosphate dehydrogenase (G6PD) and 6-gluconate phosphate dehydrogenase (6GDH) (31). While the expression level of *gspd-1* gene encoding G6PD remains unchanged, that of T25B9.9 gene encoding 6GDH, being consistent with metabolite data, reduced significantly (Figure 4). NADPH is important due to its function in cellular oxidative stress resistance and lifespan

extension. In *Drosophila*, it is reported that increase in NADPH biosynthesis, resulted in stress resistance enhancement, can extend lifespan (32). As NADPH is a substrate for Glutathione reductase (GR), which catalyzes the reduction of Glutathione disulfide (GSSG) to the sulfhydryl form Glutathione (GSH), accompanying by the release of oxidative form $NADP^+$, the decreased $NADPH/NADP^+$ ratio reflects the changes in GSH/GSSH ratio (31). It is accepted that the cellular antioxidant function of NADPH comes through its role in regeneration of GSH (33). GSH participates in many antioxidant reactions through several key enzymes including Glutathione peroxidase (GPx) and Glutathione-S-transferase (GST) (34). Interestingly, genes encoding these enzymes are down-regulated in *skn-1* knockdown worms (Figure 4), indicating the deficiency in the oxidative stress resistance in *C.elegans*.

The antioxidant effect of GSH in order to maintain the cellular redox status requires further discussion. In our data, the level of total GSH in *skn-1* RNAi worms is down-regulated. GSH can be supplied from 2 sources: regeneration from GSSG by NADPH-dependent GR enzyme and *de novo* synthesis from cysteine and glutamate (Figure 6). In *skn-1* knockdown *C.elegans,* GR function might be suppressed by the decrease of its substrate GSSG and NADPH, even though the expression level of *trxr-2* gene encoding GR remained unchanged (Table 2). Another GSH biosynthesis pathway relates to cysteine, glutamate and two enzyme γ-glutamylcisteine synthetase (GCS) and GSH synthetase (35). Cysteine is converted from homocystein, through the intermediate cystathionine in the

transsulfuration pathway. The accumulation of methionine and serine, the precursor of homocysteine and cystathionine respectively, and the low level of cystathionine suggest an impairment of this pathway in the *skn-1* RNAi worms. Transsulfuration pathway is an important source of GSH synthesis since it contributes to half of the GSH level in cell (36). This hypothesis is further confirmed with the down expression of *cbl-1* gene encoding Cystathionine γ lyase, a main enzyme in the transsulfuration pathway, in the knockdown worms. Similarly, both glutamine and glutamate level also decreased in *skn-1* RNAi worms. As a precursor of glutamate for GSH synthesis, Glutamine supplementation can increase GSH level in rat model (37). Thus, when the supply of cysteine and glutamate reduced, the two enzymes GCS and GSH synthetase might not work efficiently in *skn-1* RNAi strain, explaining for the weakness in the *de novo* synthesis of GSH. The reduction of GSH level results in failing to provide the electron for Glutathione peroxidase in scavenging the oxygen-derived free radicals. This may increase the cellular damage in *skn-1* RNAi worms, which is a potential risk of aging (34). In previous studies, it is also reported that total GSH can be considered as a predictor of aging since its level reduces significantly in aging (38) and the increase in GSH intake results in extending the *C.elegans* lifespan (39).

Since SKN-1 regulates genes belonging to the phase II detoxification system and enhancement of this system is responsible for the lifespan extension in *C.elegans* (40), we raised a possibility that knockdown of *skn-1* gene will debilitate the activity of enzymes in this pathway. In *C.elegans*, it is reported that GSTs and

UGTs are the dominant detoxification enzymes. To understand the difference of the enzyme activities at metabolite level, *C.elegans* were treated with paracetamol, a compound detoxified by phase II enzymes, and compared its glutathione conjugate between *skn-1* RNAi worms and WT. Our targeted metabolomics confirmed the decrease in the glutathione – conjugated paracetamol, a product of phase II detoxification pathway. Consistent with this result, information from microarray data also informed a down-regulation in expression of a set of genes encoding GSTs (gst-4,….) and UGTs (ugt-5,…) in *skn-1* knockdown strain (Table 2). The correlation of phase II detoxification and lifespan has been well-characterized in previous studies. In a study using rat model, we discovered that phase II reactions are required for Caloric restriction's benefits, including lifespan extension (41). In addition, the induction of Phase II detoxification by environmental stress is suppressed in aging mice (42) or depletion of SKN-1 signaling pathway occurs simultaneously with the aging development in *C.elegans* (43).

A notable feature in *skn-1* knockdown strain is the lower level of ATP resulting in the increase of AMP/ATP ratio. This ratio is a predictor of senescence in cell (44) and lifespan in *C.elegans* (45). It is reported that *C.elegans* with lower AMP/ATP live longer than those with higher AMP/ATP ratio (45). The increased AMP/ATP ratio is reported to activate cellular AMPK pathway (46). However, microarray data showed that *aak-2* encoding AMPK alpha subunit remained unchanged in *skn-1* knockdown worms. To our knowledge, there has been no study describing the relationship between SKN-1/Nrf2 and AMPK pathway in aging so far, excepting

one research characterized the intersection of these pathways in lipopolysaccharide - triggered inflammatory system (47). Thus, a full disclose of the connection between these two pathways will bring new ideas in longevity study. In addition, although ATP is mostly generated by TCA cycle in mitochondria, the metabolite and gene expression data do not reflect the significant changes in this cycle. However, genes encoding enzymes in the DNA replication and transcription such as DNA polymerase and RNA polymerase (Table 2) are up-regulated significantly in *skn-1* RNAi worms. It seems that there is an enhancement in the energy consumption for DNA and RNA synthesis, which are the material for protein translation. Increasing in energy expenditure may play a key role in life span determination, since inhibition of translation, which results in energy preservation activated the oxidative stress resistance and longevity in SKN-1- dependent manner (48).

As being reported to associate with lifespan extension, the increase of phosphocholine in the *skn-1* RNAi worms also needs to be discussed (49). Long-lived mutants *C.elegans eat-2* and *slcf-1*, which mimic the caloric restriction condition, experienced a decline in level of phosphocholine and this level, in contrast, increased significantly in short-lived *daf-18* and *daf-18, slcf-1* double mutants. Therefore, the increase of phosphocholine has been suggested as a predictor for short lifespan expectancy in *C.elegans* (50).

Collectively, by applying NMR and LC/MS – based metabolomics approach, we successfully characterized the changes in cellular metabolism of *skn-1* knockdown

worms with the noticeable decrease in the cytoprotective pathways including oxidative stress resistance and phase II detoxification system. These changes are commensurate with gene expression data published previously. Although the correlation between the oxidative stress and aging is still debated (18), recent studies have paved the way for understanding the function of cytoprotective pathway and longevity. By employing the RNAi screening to study the mechanism underlying multiple longevity pathways, knockdown of 25 in 29 genes regulating the cytoprotection were identified to reduce the lifespan of at least one long-lived mutant background (51). In addition, by examining genome-wide gene expression profiles of *C.elegans* and mouse under various caloric restriction conditions, the cellular surveillance-activated detoxification and defenses (cSADDs) pathway is also reported to have the main role in necessitating the lifespan extension (52). Thus, being consistent with other studies, our result also suggests that the impairment in the cytoprotective pathway underlies the decline of skn-1 *RNAi* worms' lifespan.

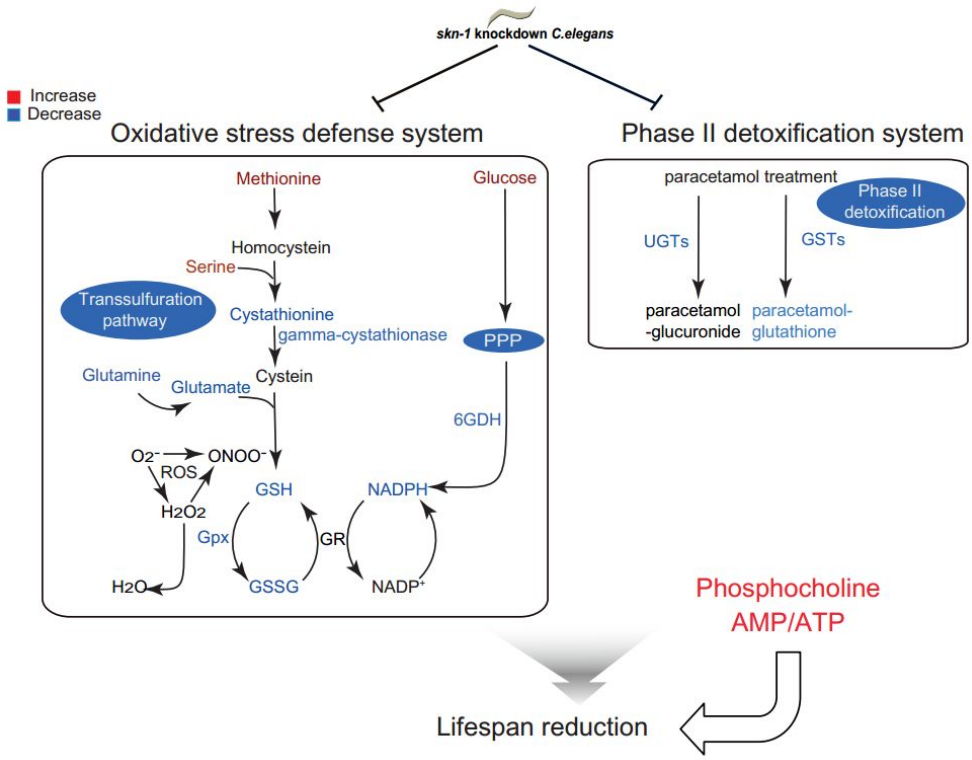

Figure 6. Overall changes in *skn-1* knockdown worms

The changes of metabolites and corresponding enzymes are indicated. Red: increase; Blue: decrease; Black: not changed or no detected.

Table 2. Gene expression level changes in skn-1 knockdown worms

Pathway	enzyme number	enzyme name	sequence name	Gene public name	Exp1(106125)	Exp2(106034)	Exp3(106036)	Mean	STDEV	Count	t-statistic	p-value
Cysteine and Methionine metabolism	2.5.1.6	S-adenosyl methionine synthetase	T13A10.11	sams-5	0.356	0.185	0.402	0.314333333	0.114343051	3	4.76147	0.04139
Cysteine and Methionine metabolism	2.5.1.6	S-adenosyl methionine synthetase	C06E7.3	sams-4	0.464	0.329	0.3115	0.368166667	0.083454079	3	7.61414	0.0167
Cysteine and Methionine metabolism	4.4.1.1	cystathionine gamma-lyase	C12C8.2	cbl-1	-0.77945	-0.6511	-0.76395	-0.7315	0.070058422	3	-18.08483732	0.00304
Starch and Sucrose metabolism	2.7.1.1	Hexokinase	F14B4.2		0.612	0.405	0.632	0.549666667	0.125683465	3	7.57499	0.01698
Pentose Phosphate	1.1.1.44	6-phosphogluconate dehydrogenase	T25B9.9		-0.0855	-0.12975	-0.194	-0.136416667	0.054556355	3	-4.330945481	0.01288
Pentose Phosphate	5.4.2.2	Phosphoglucomutase	R05F9.6		0.1865	0.0875	0.0835	0.119166667	0.058346665	3	3.53752388	0.03572564
TCA cycle	4.2.1.3	aconitate hydratase	ZK455.1	aco-1	-0.322	-0.199228621	-0.2395	-0.320242874	0.079878807	3	-6.943981165	0.01005757
TCA cycle	2.3.1.61	2-oxoglutarate dehydrogenase E2 component	W02F12.5	dlst-1	0.097	0.0405	0.083	0.0735	0.02942363	3	4.326649517	0.02473464
TCA cycle	1.1.1.37	malate dehydrogenase	F46E10.10	mdh-1	0.1035	0.1625	0.24725	0.171083333	0.072258362	3	4.100909829	0.0273173
Glycolysis/Glucuneogenesis	2.7.1.11	6-phosphofructokinase 1	C50F4.2	pfk-2	-0.0885	-0.264	-0.2375	-0.196666667	0.094607523	3	-3.600524033	0.03461202
Glycolysis/Glucuneogenesis	1.2.1.12	glyceraldehyde 3-phosphate dehydrogenase	T09F3.3	gpd-1	0.41975	0.306	0.628	0.45125	0.163294787	3	4.786361774	0.02049281
Glycolysis/Glucuneogenesis	5.4.2.12	2,3-bisphosphoglycerate-independent phosphoglycerate mutase	T07F12.1		-0.259	-0.2975	-0.443	-0.333166667	0.09704681	3	-5.946219087	0.01356828
Glycolysis/Glucuneogenesis	5.4.2.12	2,3-bisphosphoglycerate-independent phosphoglycerate mutase	Y18H1A.4		0.1695	0.0775	0.2195	0.1555	0.072027772	3	3.739306264	0.03233959
Detoxification	2.5.1.18	Glutathione S-transferase	Y45G12C.2	gst-10	-0.9415	-1.619	-1.233	-1.2645	0.339844657	3	-6.444607306	0.02324
Detoxification	2.5.1.18	Glutathione S-transferase	T26C5.1	gst-13	-1.771	-1.8165	-1.9445	-1.844	0.089959713	3	-35.50136891	0.000792
Detoxification	2.5.1.18	Glutathione S-transferase	F37B1.4	gst-15	0.2475	0.131	0.182	0.186833333	0.0584002	3	5.54115957	0.03106
Detoxification	2.5.1.18	Glutathione S-transferase	Y53F4B.19	gst-26	-0.07	-0.037	-0.0825	-0.063166667	0.023507091	3	-4.654249878	0.04319
Detoxification	2.5.1.18	Glutathione S-transferase	R07B1.4	gst-36	-0.1295	-0.2165	-0.2295	-0.191833333	0.054372174	3	-6.110939731	0.02575
Detoxification	2.5.1.18	Glutathione S-transferase	F35E8.8	gst-38	-1.727	-3.1785	-3.45	-2.785166667	0.926399257	3	-5.207312223	0.03496
Detoxification	2.5.1.18	Glutathione S-transferase	Y53F4B.33	gst-39	-0.3765	-0.423	-0.318	-0.3725	0.052614162	3	-12.26264767	0.00658
Detoxification	2.5.1.18	Glutathione S-transferase	K08F4.7	gst-4	-1.952	-2.208	-2.197	-2.119	0.144730785	3	-25.35891498	0.00155
Detoxification	2.5.1.18	Glutathione S-transferase	D1053.1	gst-42	-0.3505	-0.375	-0.299	-0.3415	0.038791107	3	-15.24822035	0.00427
Detoxification	2.5.1.18	Glutathione S-transferase	R03D7.6	gst-5	-0.621	-1.264	-0.952	-0.945666667	0.321546782	3	-5.093948386	0.03644
Detoxification	2.5.1.18	Glutathione S-transferase	F11G11.3	gst-6	-0.8305	-1.0375	-0.8885	-0.918833333	0.106781709	3	-14.90391973	0.00223588
Detoxification	2.5.1.18	Glutathione S-transferase	F11G11.2	gst-7	-0.4265	-0.2435	-0.7395	-0.469833333	0.250823311	3	-3.244416164	0.04165103
Detoxification	2.5.1.18	Glutathione S-transferase	F11G11.1	gst-8	-0.3255	-0.349	-0.6845	-0.453	0.200828907	3	-3.906902778	0.02985341
Detoxification	2.4.1.17	UDP-glucuronosyl and UDP-glucosyl transferase	2C455.4	ugt-6	-0.3785	-0.1685	-0.472	-0.339666667	0.155431925	3	-3.785064902	0.03162478
Detoxification	2.4.1.17	UDP-glucuronosyl and UDP-glucosyl transferase	T03D3.1	ugt-53	0.6235	0.7615	1.277	0.887333333	0.34444315	3	4.462003144	0.02336721
Detoxification	2.4.1.17	UDP-glucuronosyl and UDP-glucosyl transferase	2C455.6	ugt-5	-0.3975	-0.4095	-0.475	-0.427333333	0.041714306	3	-17.74362597	0.0015806
Detoxification	2.4.1.17	UDP-glucuronosyl and UDP-glucosyl transferase	C18C4.3	ugt-48	-0.383	-0.285	-0.435	-0.367666667	0.076166484	3	-4.360860457	0.00700276
Detoxification	2.4.1.17	UDP-glucuronosyl and UDP-glucosyl transferase	B0310.5	ugt-46	-0.2125	-0.4315	-0.177	-0.273666667	0.137835349	3	-3.438918795	0.03757522
Detoxification	2.4.1.17	UDP-glucuronosyl and UDP-glucosyl transferase	F01D4.1	ugt-43	-0.341	-0.226	-0.496	-0.354333333	0.135492927	3	-4.529559946	0.02272181
Detoxification	2.4.1.17	UDP-glucuronosyl and UDP-glucosyl transferase	2C455.5	ugt-4	-0.157	-0.1225	-0.3325	-0.204	0.112613276	3	-3.137626187	0.04416338
Detoxification	2.4.1.17	UDP-glucuronosyl and UDP-glucosyl transferase	F10D2.6	ugt-37	-0.254	-0.152	-0.1185	-0.174833333	0.07057679	3	-4.290648736	0.0251297
Detoxification	2.4.1.17	UDP-glucuronosyl and UDP-glucosyl transferase	F09G2.6	ugt-36	-0.2985	-0.1775	-0.202	-0.226	0.063970696	3	-6.11910616	0.01284127
Detoxification	2.4.1.17	UDP-glucuronosyl and UDP-glucosyl transferase	C35A5.2	ugt-33	-0.363	-0.2965	-0.737	-0.4655	0.237465261	3	-3.395316219	0.03843734
Detoxification	2.4.1.17	UDP-glucuronosyl and UDP-glucosyl transferase	Y39G10AR.6	ugt-31	-0.665	-0.8855	-0.254	-0.6015	0.32050312	3	-3.25060349	0.0415118
Detoxification	2.4.1.17	UDP-glucuronosyl and UDP-glucosyl transferase	C17G1.3	ugt-23	-0.4035	-0.2165	-0.325	-0.315	0.093900213	3	-5.810380903	0.01418306
Detoxification	2.4.1.17	UDP-glucuronosyl and UDP-glucosyl transferase	C08F11.8	ugt-22	-0.911	-0.9435	-0.875	-0.909833333	0.034264899	3	-45.99101663	0.00023622
Detoxification	2.4.1.17	UDP-glucuronosyl and UDP-glucosyl transferase	2C443.6	ugt-16	-0.7575	-0.8145	-0.7555	-0.775833333	0.033501244	3	-40.11142874	0.00031048
Detoxification	2.4.1.17	UDP-glucuronosyl and UDP-glucosyl transferase	AC3.7	ugt-1	-0.44905	-1.01	-0.91355	-0.790866667	0.299924367	3	-4.567222274	0.02237329
Purine metabolism	2.7.4.6	nucleoside-diphosphate kinase	F42G9.9	ptk-1	-0.344	-0.125	-0.1805	-0.2165	0.113851877	3	-3.293656707	0.04056125
Purine metabolism	1.17.4.1	ribonucleoside-diphosphate reductase subunit M2	C03C10.3	rnr-2	0.4575	0.353	0.7055	0.505333333	0.181052709	3	4.834299439	0.02011248
Purine metabolism	1.17.4.1	ribonucleoside-diphosphate reductase subunit M1	T23G5.1	rnr-1	0.618	0.327	0.783	0.576	0.230883087	3	4.321066895	0.02480294
Purine metabolism	2.7.7.8	polyribonucleotide nucleotidyltransferase	R04D3.2		0.58	0.754	0.757	0.530333333	0.255151589	3	3.600072734	0.03461982
Purine metabolism	2.7.7.8	polyribonucleotide nucleotidyltransferase	B0205.8		0.202	0.167	0.274	0.214333333	0.054555782	3	6.804709061	0.01046052
Purine metabolism	2.7.7.7	DNA polymerase epsilon subunit 2	F08B4.5	pole-2	0.161	0.2735	0.389	0.2745	0.114003289	3	4.170475686	0.02648408
Purine metabolism	2.7.7.7	DNA polymerase delta subunit 1	F10C2.4		0.3785	0.176	0.517	0.357166667	0.171498056	3	3.607217636	0.03449667
Purine metabolism	2.7.7.7	DNA primase small subunit	F58A4.4	pri-1	0.4605	0.2085	0.6625	0.443833333	0.227458421	3	3.379702891	0.03875298
Purine metabolism	2.7.7.7	DNA polymerase delta subunit 3	R04F11.3		0.1015	0.3545	0.347	0.267666667	0.143953407	3	3.220571686	0.04219389
Purine metabolism	2.7.7.6	DNA-directed RNA polymerases I, II, and III subunit RPABC2	C06A1.5	rpb-6	0.139	0.165	0.3055	0.203166667	0.089571666	3	3.928641781	0.02955257
Purine metabolism	2.7.7.6	DNA-directed RNA polymerase III subunit RPC1	C42D4.8	rpc-1	0.38	0.1775	0.559	0.372166667	0.190870593	3	3.377217857	0.03880356
Purine metabolism	2.7.7.6	DNA-directed RNA polymerase I subunit RPA2	F14B4.3	rpoa-2	0.174	0.201	0.4245	0.2665	0.137496364	3	3.35718168	0.0392162
Purine metabolism	2.7.7.6	DNA-directed RNA polymerase II subunit RPB4	F43E2.2	rpb-4	0.369	0.176	0.464	0.336333333	0.146752626	3	3.969580894	0.02899788
Purine metabolism	2.7.7.6	DNA-directed RNA polymerases I and III subunit RPAC2	F58A4.9	rpac-19	0.104	0.157	0.1075	0.122833333	0.029640906	3	7.177701356	0.00943136
Purine metabolism	2.7.7.6	DNA-directed RNA polymerases I, II, and III subunit RPABC1	H27M09.2	rpb-5	0.1655	0.2	0.301	0.222166667	0.070417209	3	5.464629449	0.01594689
Purine metabolism	2.7.7.6	DNA-directed RNA polymerases I and III subunit RPAC1	H43I07.2	rpac-40	0.1625	0.099	0.174	0.145166667	0.040392862	3	6.22476416	0.01242502
Purine metabolism	2.7.7.6	DNA-directed RNA polymerase III subunit RPC6	W09C3.4		0.2575	0.0785	0.2635	0.199833333	0.105120566	3	3.292614381	0.04058389
Purine metabolism	2.7.7.6	DNA-directed RNA polymerase II subunit RPB7	Y54E10BR.6	rpb-7	0.2485	0.163	0.292	0.2345	0.065629643	3	6.188757057	0.0125646
Purine metabolism	2.7.7.6	DNA-directed RNA polymerase III subunit RPC8	ZK856.10	rpc-25	0.21	0.198	0.3085	0.238833333	0.060630713	3	6.822803969	0.01040682
Glycerophospholipid metabolism	2.3.1.6	Choline acetyltransfrase	F55A4.8		-0.19125	-0.16975	-0.199	-0.253333333	0.126608238	3	-3.46570028	0.03705945
Lipid metabolism	6.2.1.3	Long-chain fatty-acid CoA ligase	F28F8.2	acs-2	0.672	0.007	0.387	0.355333333	0.333629036	3	1.844729689	0.06941748
Glutathione metabolism	1.11.1.9	Glutathione peroxidase	F26E4.12	gpx-1	-0.399	-0.7815	-0.524	-0.568166667	0.19503739	3	-5.045666044	0.01855336
Glutathione metabolism	1.11.1.9	Glutathione peroxidase	R03G5.5	gpx-7	-0.622	-0.4765	-0.572	-0.556833333	0.073926202	3	-13.04630293	0.00291198

References

1. Leiser, S. F., and Miller, R. A. (2010) Nrf2 signaling, a mechanism for cellular stress resistance in long-lived mice. *Molecular and cellular biology* 30, 871-884

2. Mukaigasa, K., Nguyen, L. T., Li, L., Nakajima, H., Yamamoto, M., and Kobayashi, M. (2012) Genetic evidence of an evolutionarily conserved role for Nrf2 in the protection against oxidative stress. *Molecular and cellular biology* 32, 4455-4461

3. An, J. H., and Blackwell, T. K. (2003) SKN-1 links C. elegans mesendodermal specification to a conserved oxidative stress response. *Genes & Development* 17, 1882-1893

4. An, J. H., Vranas, K., Lucke, M., Inoue, H., Hisamoto, N., Matsumoto, K., and Blackwell, T. K. (2005) Regulation of the Caenorhabditis elegans oxidative stress defense protein SKN-1 by glycogen synthase kinase-3. *Proceedings of the National Academy of Sciences of the United States of America* 102, 16275-16280

5. Sykiotis, G. P., and Bohmann, D. (2008) Keap1/Nrf2 Signaling Regulates Oxidative Stress Tolerance and Lifespan in Drosophila. *Developmental cell* 14, 76-85

6. Yang, Y., Cai, X., Yang, J., Sun, X., Hu, C., Yan, Z., Xu, X., Lu, W., Wang, X., and Cao, P. (2014) Chemoprevention of dietary digitoflavone on colitis-

associated colon tumorigenesis through inducing Nrf2 signaling pathway and inhibition of inflammation. *Mol Cancer* 13, 1476-4598

7. Ramos-Gomez, M., Kwak, M. K., Dolan, P. M., Itoh, K., Yamamoto, M., Talalay, P., and Kensler, T. W. (2001) Sensitivity to carcinogenesis is increased and chemoprotective efficacy of enzyme inducers is lost in nrf2 transcription factor-deficient mice. *Proceedings of the National Academy of Sciences of the United States of America* 98, 3410-3415

8. Pearson, K. J., Lewis, K. N., Price, N. L., Chang, J. W., Perez, E., Cascajo, M. V., Tamashiro, K. L., Poosala, S., Csiszar, A., Ungvari, Z., Kensler, T. W., Yamamoto, M., Egan, J. M., Longo, D. L., Ingram, D. K., Navas, P., and de Cabo, R. (2008) Nrf2 mediates cancer protection but not prolongevity induced by caloric restriction. *Proceedings of the National Academy of Sciences* 105, 2325-2330

9. Bishop, N. A., and Guarente, L. (2007) Two neurons mediate diet-restriction-induced longevity in C. elegans. *Nature* 447, 545-549

10. Okuyama, T., Inoue, H., Ookuma, S., Satoh, T., Kano, K., Honjoh, S., Hisamoto, N., Matsumoto, K., and Nishida, E. (2010) The ERK-MAPK pathway regulates longevity through SKN-1 and insulin-like signaling in Caenorhabditis elegans. *The Journal of biological chemistry* 285, 30274-30281

11. Tullet, J. M., Hertweck, M., An, J. H., Baker, J., Hwang, J. Y., Liu, S., Oliveira, R. P., Baumeister, R., and Blackwell, T. K. (2008) Direct inhibition of the longevity-promoting factor SKN-1 by insulin-like signaling in C. elegans. *Cell* 132, 1025-1038

12. Oliveira, R. P., Porter Abate, J., Dilks, K., Landis, J., Ashraf, J., Murphy, C. T., and Blackwell, T. K. (2009) Condition-adapted stress and longevity gene regulation by Caenorhabditis elegans SKN-1/Nrf detoxification enzymes up-regulated by SKN-1 under normal condition. *Aging cell* 8, 524-541

13. Motohashi, H., and Yamamoto, M. (2004) Nrf2–Keap1 defines a physiologically important stress response mechanism. *Trends in Molecular Medicine* 10, 549-557

14. Lindblom, T. H., and Dodd, A. K. (2006) Xenobiotic detoxification in the nematode Caenorhabditis elegans. *Journal of experimental zoology. Part A, Comparative experimental biology* 305, 720-730

15. Lee, J. M., Li, J., Johnson, D. A., Stein, T. D., Kraft, A. D., Calkins, M. J., Jakel, R. J., and Johnson, J. A. (2005) Nrf2, a multi-organ protector? *FASEB journal : official publication of the Federation of American Societies for Experimental Biology* 19, 1061-1066

16. Jakoby, W. B., and Ziegler, D. M. (1990) The enzymes of detoxication. *Journal of Biological Chemistry* 265, 20715-20718

17. Park, S. K., Tedesco, P. M., and Johnson, T. E. (2009) Oxidative stress and longevity in Caenorhabditis elegans as mediated by SKN-1. *Aging cell* 8, 258-269

18. Back, P., Braeckman, B. P., and Matthijssens, F. (2012) ROS in aging Caenorhabditis elegans: damage or signaling? *Oxidative medicine and cellular longevity* 2012, 608478

19. Johnson, T. E., de Castro, E., Hegi de Castro, S., Cypser, J., Henderson, S., and Tedesco, P. (2001) Relationship between increased longevity and stress resistance as assessed through gerontogene mutations in Caenorhabditis elegans. *Experimental gerontology* 36, 1609-1617

20. Patti, G. J., Yanes, O., and Siuzdak, G. (2012) Innovation: Metabolomics: the apogee of the omics trilogy. *Nature reviews. Molecular cell biology* 13, 263-269

21. Fuchs, S., Bundy, J. G., Davies, S. K., Viney, J. M., Swire, J. S., and Leroi, A. M. (2010) A metabolic signature of long life in Caenorhabditis elegans. *BMC biology* 8, 14

22. Blaise, B. J., Giacomotto, J., Elena, B., Dumas, M. E., Toulhoat, P., Segalat, L., and Emsley, L. (2007) Metabotyping of Caenorhabditis elegans reveals latent phenotypes. *Proceedings of the National Academy of Sciences of the United States of America* 104, 19808-19812

23. Swire, J., Fuchs, S., Bundy, J. G., and Leroi, A. M. (2009) The cellular geometry of growth drives the amino acid economy of Caenorhabditis elegans. *Proceedings. Biological sciences / The Royal Society* 276, 2747-2754

24. Ratcliffe, R. G., and Shachar-Hill, Y. (2001) Probing plant metabolism with NMR. *Annual review of plant biology* 52, 499-526

25. Kikuchi, J., Shinozaki, K., and Hirayama, T. (2004) Stable isotope labeling of Arabidopsis thaliana for an NMR-based metabolomics approach. *Plant & cell physiology* 45, 1099-1104

26. Sekiyama, Y., Chikayama, E., and Kikuchi, J. (2011) Evaluation of a semipolar solvent system as a step toward heteronuclear multidimensional NMR-based metabolomics for 13C-labeled bacteria, plants, and animals. *Anal Chem* 83, 719-726

27. An, Y. J., Xu, W. J., Jin, X., Wen, H., Kim, H., Lee, J., and Park, S. (2012) Metabotyping of the C. elegans sir-2.1 mutant using in vivo labeling and (13)C-heteronuclear multidimensional NMR metabolomics. *ACS chemical biology* 7, 2012-2018

28. Kamath, R. S., Fraser, A. G., Dong, Y., Poulin, G., Durbin, R., Gotta, M., Kanapin, A., Le Bot, N., Moreno, S., Sohrmann, M., Welchman, D. P., Zipperlen, P., and Ahringer, J. (2003) Systematic functional analysis of the Caenorhabditis elegans genome using RNAi. *Nature* 421, 231-237

29. Braeckman, B. P., Houthoofd, K., De Vreese, A., and Vanfleteren, J. R. (2002) Assaying metabolic activity in ageing Caenorhabditis elegans. *Mechanisms of ageing and development* 123, 105-119

30. Chikayama, E., Sekiyama, Y., Okamoto, M., Nakanishi, Y., Tsuboi, Y., Akiyama, K., Saito, K., Shinozaki, K., and Kikuchi, J. (2010) Statistical indices for simultaneous large-scale metabolite detections for a single NMR spectrum. *Anal Chem* 82, 1653-1658

31. Ying, W. (2008) NAD+/NADH and NADP+/NADPH in cellular functions and cell death: regulation and biological consequences. *Antioxidants & redox signaling* 10, 179-206

32. Legan, S. K., Rebrin, I., Mockett, R. J., Radyuk, S. N., Klichko, V. I., Sohal, R. S., and Orr, W. C. (2008) Overexpression of Glucose-6-phosphate Dehydrogenase Extends the Life Span of Drosophila melanogaster. *Journal of Biological Chemistry* 283, 32492-32499

33. Holmgren, A., Johansson, C., Berndt, C., Lonn, M., Hudemann, C., and Lillig, C. (2005) Thiol redox control via thioredoxin and glutaredoxin systems. *Biochemical Society Transactions* 33, 1375-1377

34. Wu, G., Fang, Y. Z., Yang, S., Lupton, J. R., and Turner, N. D. (2004) Glutathione metabolism and its implications for health. *J Nutr* 134, 489-492

35. Brown-Borg, H. M. (2006) Longevity in mice: is stress resistance a common factor? *Age (Dordr)* 28, 145-162

36. Mosharov, E., Cranford, M. R., and Banerjee, R. (2000) The Quantitatively Important Relationship between Homocysteine Metabolism and Glutathione Synthesis by the Transsulfuration Pathway and Its Regulation by Redox Changes†. *Biochemistry* 39, 13005-13011

37. Johnson, A. T., Kaufmann, Y. C., Luo, S., Todorova, V., and Klimberg, V. S. (2003) Effect of glutamine on glutathione, IGF-I, and TGF-β1. *Journal of Surgical Research* 111, 222-228

38. Samiec, P. S., Drews-Botsch, C., Flagg, E. W., Kurtz, J. C., Sternberg Jr, P., Reed, R. L., and Jones, D. P. (1998) Glutathione in Human Plasma: Decline in Association with Aging, Age-Related Macular Degeneration, and Diabetes. *Free Radical Biology and Medicine* 24, 699-704

39. Cascella, R., Evangelisti, E., Zampagni, M., Becatti, M., D′Adamio, G., Goti, A., Liguri, G., Fiorillo, C., and Cecchi, C. (2014) S-linolenoyl glutathione intake extends life-span and stress resistance via Sir-2.1 upregulation in Caenorhabditis elegans. *Free Radical Biology and Medicine* 73, 127-135

40. McElwee, J. J., Schuster, E., Blanc, E., Thomas, J. H., and Gems, D. (2004) Shared transcriptional signature in Caenorhabditis elegans Dauer larvae and long-lived daf-2 mutants implicates detoxification system in longevity assurance. *The Journal of biological chemistry* 279, 44533-44543

41. Wen, H., Yang, H. J., An, Y. J., Kim, J. M., Lee, D. H., Jin, X., Park, S. W., Min, K. J., and Park, S. (2013) Enhanced phase II detoxification contributes to beneficial effects of dietary restriction as revealed by multi-platform metabolomics studies. *Mol Cell Proteomics* 12, 575-586

42. Zhang, H., Liu, H., Davies, K. J., Sioutas, C., Finch, C. E., Morgan, T. E., and Forman, H. J. (2012) Nrf2-regulated phase II enzymes are induced by chronic ambient nanoparticle exposure in young mice with age-related impairments. *Free radical biology & medicine* 52, 2038-2046

43. Przybysz, A. J., Choe, K. P., Roberts, L. J., and Strange, K. (2009) Increased age reduces DAF-16 and SKN-1 signaling and the hormetic response of Caenorhabditis elegans to the xenobiotic juglone. *Mechanisms of ageing and development* 130, 357-369

44. Wang, W., Yang, X., López de Silanes, I., Carling, D., and Gorospe, M. (2003) Increased AMP:ATP Ratio and AMP-activated Protein Kinase Activity

during Cellular Senescence Linked to Reduced HuR Function. *Journal of Biological Chemistry* 278, 27016-27023

45. Apfeld, J., O'Connor, G., McDonagh, T., DiStefano, P. S., and Curtis, R. (2004) The AMP-activated protein kinase AAK-2 links energy levels and insulin-like signals to lifespan in C. elegans. *Genes & Development* 18, 3004-3009

46. Hardie, D. G., Ross, F. A., and Hawley, S. A. (2012) AMPK: a nutrient and energy sensor that maintains energy homeostasis. *Nature reviews. Molecular cell biology* 13, 251-262

47. Mo, C., Wang, L., Zhang, J., Numazawa, S., Tang, H., Tang, X., Han, X., Li, J., Yang, M., Wang, Z., Wei, D., and Xiao, H. (2014) The crosstalk between Nrf2 and AMPK signal pathways is important for the anti-inflammatory effect of berberine in LPS-stimulated macrophages and endotoxin-shocked mice. *Antioxidants & redox signaling* 20, 574-588

48. Wang, J., Robida-Stubbs, S., Tullet, J. M. A., Rual, J.-F., Vidal, M., and Blackwell, T. K. (2010) RNAi Screening Implicates a SKN-1–Dependent Transcriptional Response in Stress Resistance and Longevity Deriving from Translation Inhibition. *PLoS genetics* 6, e1001048

49. Patti, G., Tautenhahn, R., Johannsen, D., Kalisiak, E., Ravussin, E., Brüning, J., Dillin, A., and Siuzdak, G. (2014) Meta-analysis of global metabolomic data identifies metabolites associated with life-span extension. *Metabolomics* 10, 737-743

50. Pontoizeau, C., Mouchiroud, L., Molin, L., Mergoud-Dit-Lamarche, A., Dalliere, N., Toulhoat, P., Elena-Herrmann, B., and Solari, F. (2014) Metabolomics analysis uncovers that dietary restriction buffers metabolic changes associated with aging in Caenorhabditis elegans. *J Proteome Res* 13, 2910-2919

51. Shore, D. E., Carr, C. E., and Ruvkun, G. (2012) Induction of cytoprotective pathways is central to the extension of lifespan conferred by multiple longevity pathways. *PLoS genetics* 8, e1002792

52. Ludewig, A. H., Klapper, M., and Doring, F. (2014) Identifying evolutionarily conserved genes in the dietary restriction response using bioinformatics and subsequent testing in Caenorhabditis elegans. *Genes Nutr* 9, 013-0363

국문초록

C.elegans 에서

skn-1 down-regulation 의

대사체학적 효과

Phan Chau Hong Duc

서울대학교 약학대학원

약학과 천연물과학전공

SKN-1/Nrf2는 산화스트레스 내성 매커니즘과 해독 경로를 활성화시킨다고 잘 알려져 있는 전사인자로서 *C.elegans*에서는 또한 *C.elegans*의 수명에 영향을 준다고 입증되어 왔다. 많은 연구들이 *skn-1* 의 유전자 수준에서의 기능만을 다루어 온 반면, 개별적인 대사체에 대한 체계적인 연구는 부족한 실정이다. SKN-1의 기능이 대사와 관련이 있기 때문에 우리는 *skn-1* 을 knockdown시킨 *C.elegans* 의 대사 프로파일을 NMR과 LC-MS/MS를 이용한 대사체학적 접근을 통해서 확인하였다. Multivariate analysis를

사용하여 *skn-1* RNAi *C.elegans*에서 NADPH/$NADP^+$비율의 감소로 대변되는 산화 스트레스 저항 시스템의 현저한 감소, GSH 합성의 주요한 원천이 되는 황전환작용 경로의 감소, 그리고 전체 GSH 레벨의 감소와 같은 뚜렷한 대사 프로파일을 확인하였다. 우리는 phase II 해독 경로를 통해 해독되는 paracetamol의 glutathione conjugate 레벨이 감소되는 것으로 보아 phase II 해독 경로에 손상이 있음을 제안할 수 있었다. 게다가 우리는 기존에 발표된 microarray data의 정보를 분석하여 대사체 data의 변화가 유전자 발현 레벨과 일관성이 있음을 관찰할 수 있었다. 일관성을 보인 유전자 발현 레벨은 각각 GSH의 합성과 기능에 필수적인 γ-cystathionase와 glutathione peroxidase을 인코딩하는 *cbl-1*과 *gpx*의 감소, NADPH를 생산하는 주요 효소인 6-gluconate phosphate dehydrogenase를 인코딩하는 T25B9.9이 감소, 그리고 phase II 해독 경로에서 기능을 하는 UDP-glucuronosyl transferase와 Glutathione-S-transferase를 인코딩하는 *ugt*와 *gst*의 감소였다. 노화와 산화적 손상 사이에 연관이 있다는 기존의 가설과 유사하게 우리는 산화스트레스 방어 시스템과 생체 이물 해독 시스템을 포함하는 세포보호 경로의 약화가 *skn-1* knockdown *C.elegans*의 수명 단축에 기여할 수 있다는 결론을 얻었다.

주요어: *skn-1*, phase II 해독경로, 예쁜꼬마선충, 대사체학

학번: 2013-22584